

## Net ecosystem production of dissolved organic carbon in a coastal upwelling system: the Ría de Vigo, Iberian margin of the North Atlantic

X. A. Álvarez-Salgado and J. Gago

CSIC, Instituto de Investigaciones Mariñas, Eduardo Cabello 6, 36208–Vigo, Spain

B. M. Míguez

Facultad de Ciencias del Mar, Universidad de Vigo, apartado 874, 36200–Vigo, Spain

F. F. Pérez

CSIC, Instituto de Investigaciones Mariñas, Eduardo Cabello 6, 36208–Vigo, Spain

### Abstract

Net ecosystem production (NEP) rates of dissolved organic carbon (DOC) are estimated in a coastal upwelling system. The study site is a large coastal inlet ( $2.76 \text{ km}^3$ ) in the northern boundary ( $42\text{--}43^\circ\text{N}$ ) of the eastern North Atlantic upwelling system. The two-dimensional circulation pattern in the system is governed by an offshore Ekman transport quite variable in magnitude and direction. A mass balance of the short-timescale (2–4 d) changes in measured DOC profiles is performed to obtain the NEP rates. Microbial oxidation of imported labile DOC (8% of total DOC, recycling time  $\tau < 5$  d) at a maximum net rate of  $-37 \text{ mmol C m}^{-2} \text{ d}^{-1}$  occurred during a downwelling episode in the middle of the highly productive spring period. On the contrary, extensive export of labile DOC (<15% of total DOC,  $\tau < 7$  days) produced at net rates  $>42 \text{ mmol C m}^{-2} \text{ d}^{-1}$  took place during an upwelling episode in July, the middle of the upwelling season. This rate represents  $\sim 20\%$  of the net primary production, demonstrating in the field the relative importance of horizontal offshore transport of labile DOC to the export of new production in upwelling systems. An autumn wind relaxation period results in dramatic changes in DOC standing stocks ( $\pm 9 \mu\text{mol C L}^{-1}$ ) caused by a conspicuous time segregation between sustained net phytoplankton production of labile DOC ( $+15 \text{ mmol C m}^{-2} \text{ d}^{-1}$ , 11 d) and subsequent rapid bacterial degradation ( $-63 \text{ mmol C m}^{-2} \text{ d}^{-1}$ , 3 d). Net horizontal export during this period was prevented by reduced offshore Ekman transport values, indicating that net DOC production is not always synonymous with net export. Finally, during the winter period, the large wind-driven net DOC horizontal exchange rates affected mainly the DOC standing stocks of no bioreactive materials in the system, whereas bacterial oxidation rates during this period reduced to less than  $-0.14 \text{ mmol C m}^{-2} \text{ d}^{-1}$ .

Incorporation of the phylogenetic bioreactive fractions of dissolved organic matter (DOM) in experimental (Carlson et al. 1994) and modeling (Anderson and Williams 1999) approaches to carbon cycling have advanced our understanding of the fate of primary production in the oceans. The bioreactive DOM with recycling times shorter than residence times in the study system—the labile fraction—will contribute to the regenerated production. The dimensions of the system (local to global) will dictate the timescales (days to months) involved. The bioreactive DOM with recycling times larger than residence times—the semilabile fraction—will contribute to the export production, which equals new production under steady-state conditions. Therefore, the early Eppley and Peterson (1979) concept of new production has been revisited because of the major contribution of DOM to organic matter export (Bronk et al. 1994).

### Acknowledgements

The authors thank the captain and crew of the R/V *Mytilus* and the members of the IIM Group of Oceanography for their help during the sampling programme. M. V. González assisted us in the preparation of figures. Comments by K. Soetaert have contributed to improve the manuscript.

Financial support for this work came from CICYT grant AMB95-1084. Fellowships from the Spanish Ministerio de Educación y Ciencia funded J. Gago and B. Míguez in carrying out this work.

Local downward export during winter mixing is the fate of semilabile DOM accumulated in the surface layer of areas where convective mixing succeeds summer stratification. This is the case of the northwest Mediterranean (Copin-Montégut and Avril 1993) or the Sargasso Sea (Carlson et al. 1994). In contrast, horizontal transport of semilabile DOM occurs from the eutrophic equatorial Pacific to the adjacent oligotrophic subtropical gyres (Hansell and Waterhouse 1997). Intensified horizontal flows in ocean margins must contribute significantly to the export of shelf primary production toward the adjacent ocean via semilabile DOM. Therefore, bioreactive DOM has to be incorporated in the unclosed controversy about the relative importance of export and in situ oxidation of organic matter produced in continental shelves (e.g., Walsh et al. 1988; Biscaye et al. 1994). Primary production and export of phylogenetic materials are enhanced in coastal upwelling regions, in response to the magnified shelf-edge exchange caused by the offshore Ekman transport (Walsh 1991; Wollast 1993).

Despite their relevance to global productivity and export, few studies have been conducted on the role of bioreactive DOM in coastal upwelling areas. In fact, these studies are circumscribed to the western coast of the Iberian Peninsula, the northern limit of the northwest Africa upwelling system (Doval et al. 1997; Álvarez-Salgado et al. 1999). The Rías

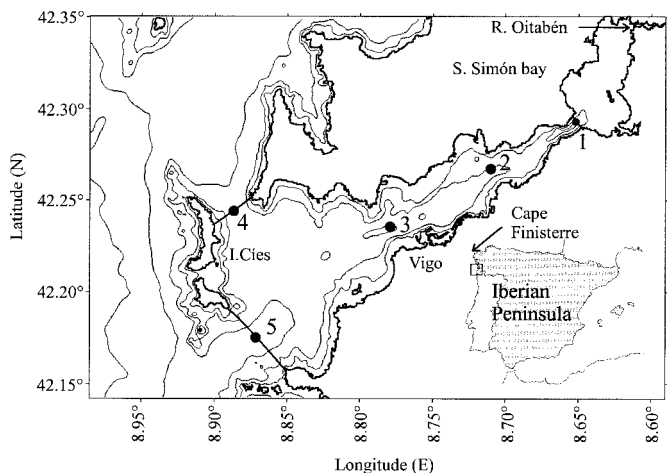


Fig. 1. Chart of the survey area (Ría de Vigo, Iberian upwelling system), showing the five sampling sites distributed along the embayment. The inner (Sta. 1) and outer (Stas. 4 and 5) boundaries delimit the study system.

Baixas—four large V-shaped indentations there—constitute a unique “macrocosms” to study the short-timescale response of the carbon cycle to shelf wind-stress. The Ekman transport controls the extremely variable short-timescale two-dimensional circulation pattern of the Rías Baixas (Rosón et al. 1997), either during the upwelling- (April–October) or the downwelling-favorable (November–March) seasons (Wooster et al. 1976; Bakun and Nelson 1991). The inorganic carbon and nutrients balances for the entire ecosystem are also subject to Ekman transport control (Pérez et al. 2000). The recent studies of Doval et al. (1997) and Álvarez-Salgado et al. (1999) describe the Rías Baixas as the preeminent site of formation for the bioreactive DOM excess observed in shelf surface waters during the upwelling season.

The present work complements the previous studies on the seasonal variation of DOM by focusing on the short-timescale (half-week) changes in the net ecosystem production (NEP) of bioreactive dissolved organic carbon (DOC) in the Ría de Vigo (northwest Spain). The relative importance of accumulation versus export under contrasting hydrographic conditions during four seasons will be examined in detail. NEP of bioreactive DOC—i.e., the DOC balance of production minus consumption for the entire ecosystem (Smith and Hollibaugh 1997)—will be estimated with a biogeochemical box model successfully applied to the adjacent Ría de Arousa (e.g., Pérez et al. 2000).

## Material and methods

**The sampling program**—An intensive hydrographic sampling was executed in the Ría de Vigo during four contrasting periods in 1997: 7–23 April, 1–18 July, 15 September–2 October, and 1–11 December. Five fixed stations were occupied—four along the main axis of the embayment and one at the shallower entrance, north of the Isles Cies (Fig. 1). Full-depth continuous conductivity-temperature-depth (CTD) profiles were recorded at each sampling site with a

SBE 25 CTD device. Conductivity measurements were converted into practical salinity scale values (UNESCO 1985). Subsequently, seawater samples for salinity analysis with a Guideline AUTOSAL 8400A and DOC determination with a Shimadzu TOC-5000 analyzer were collected from 3 to 5 depths with 5-liter Niskin bottles. This program was repeated every 2–4 d during the four sampling periods, the appropriate frequency to study the coupling between meteorological forcing and hydrography at the short timescale (Rosón et al. 1997). A total of 22 surveys were performed: 6 during the spring, summer, and autumn, and 4 during the winter period.

Daily Ekman transport values ( $-\bar{Q}_x$ ) have been calculated according to Wooster et al. (1976):

$$-\bar{Q}_x = \frac{\rho_{\text{air}} \times C \times |V| \times V_N}{\rho_{\text{sw}} \times f}, \quad (1)$$

where  $\rho_{\text{air}}$  is the density of air,  $1.22 \text{ kg m}^{-3}$  at  $15^\circ\text{C}$ ;  $C$  is an empirical drag coefficient (dimensionless),  $1.3 \times 10^{-3}$ ;  $f$  is the Coriolis parameter,  $9.946 \times 10^{-5} \text{ s}^{-1}$  at  $43^\circ$  latitude;  $\rho_{\text{sw}}$  is the density of seawater,  $\sim 1025 \text{ kg m}^{-3}$ ;  $|V|$  is wind speed; and  $V_N$  is the north component of wind speed. Wind data were taken at the Cape Finisterre Meteorological Observatory.

**DOC determination by high-temperature catalytic oxidation**—Samples for the analyses of DOC were collected into 250-ml acid-cleaned all-glass flasks. They were immediately filtered through 47-mm  $\varnothing$  Whatman GF/F filters (ashed  $450^\circ\text{C}$ , 4 h) in an acid-cleaned all-glass filtration system, and collected in 10-ml glass ampoules (ashed  $450^\circ\text{C}$ , 12 h). After acidification with  $\text{H}_3\text{PO}_4$  to  $\text{pH} < 2$ , the ampoules were heat-sealed and stored in the dark at  $4^\circ\text{C}$  until analyzed in the laboratory. DOC content in samples was measured with a commercial Shimadzu TOC-5000 organic carbon analyzer, working under the principle of high-temperature catalytic oxidation. After decarbonation of the sample by vigorous stirring with high-purity synthetic air for 15 min, 200  $\mu\text{l}$  were injected into the vertical furnace of the analyzer, filled with a conditioned 0.5% Pt-coated  $\text{Al}_2\text{O}_3$  catalyst at  $680^\circ\text{C}$ . Conditioning consisted of washing the catalyst by repetitive injections of Milli-Q water until the blank was low and stable. Quantitative production of  $\text{CO}_2$  occurs from the DOC in the sample. High-purity synthetic air carries the combustion products through a series of scrubbers (25%  $\text{H}_3\text{PO}_4$  solution, in-built Peltier cooler at  $\sim 1^\circ\text{C}$ , halogen scrubber, and particle filter) before the dried gas mixture enters the measuring cell of the Shimadzu Infrared gas analyzer. The system was standardized daily with potassium hydrogen phthalate in milli-Q water. The concentration of DOC was determined by subtracting the system blank area from the average peak area and dividing by the slope of the standard curve. The system blank—obtained by frequent injection (every 4–6 samples) of UV-Milli-Q water—was equivalent to  $5\text{--}10 \mu\text{mol C L}^{-1}$ . The precision of measurements was  $< 1\%$ , i.e.,  $\pm 0.5 \mu\text{mol C L}^{-1}$ . The accuracy of our DOC measurements were tested daily with the TOC reference materials provided by J. Sharp (University of Delaware), with very satisfactory results. We obtained an average concentration of  $45.4 \pm 1.1 \mu\text{mol C L}^{-1}$  ( $n = 44$ ) for the deep ocean reference (Sargasso Sea deep water, 2600 m) and  $0.4 \pm 0.7$

Table 1. Glossary of relevant terms used throughout the text.

$\bar{\beta}/\bar{\alpha}$	Average ratio of the coefficients of haline contraction and thermal expansion at the boundaries of system between two consecutive surveys
$\frac{\text{DOC}, \text{DOM}}{\overline{\text{DOC}}_B, \overline{\text{DOC}}_S}$	Dissolved organic carbon, dissolved organic matter Average DOC concentration in the bottom and surface layers at the boundaries of the system between two consecutive surveys
$\overline{\text{DOC}}_R, \overline{\text{DOC}}_W$	Average DOC concentration in the river discharge ( $400 \mu\text{mol C L}^{-1}$ ) and the sewage from the city of Vigo ( $3.6 \cdot 10^3 \mu\text{mol C L}^{-1}$ )
$\bar{E}$	Average evaporation between two consecutive surveys
ENACW	Eastern North Atlantic central water
$\bar{H}$	Average heat exchange flux across the air–sea interface between two consecutive surveys
$\overline{\text{NEP}}$	Average net ecosystem production of DOC between two consecutive surveys
$O - I$	Balance of DOC outputs minus inputs between two consecutive surveys
$\bar{P}$	Average precipitation between two consecutive surveys
$\bar{Q}_B, \bar{Q}_S$	Average bottom and surface horizontal convective water flux at the boundaries of the system between two consecutive surveys
$\overline{Q_B \times S_B}, \overline{Q_S \times S_S}$	Average bottom and surface horizontal convective salt flux at the boundaries of the system between two consecutive surveys
$\overline{Q_B \times T_B}, \overline{Q_S \times T_S}$	Average bottom and surface horizontal convective heat flux at the boundaries of the system between two consecutive surveys
$-\bar{Q}_x$	Average offshore Ekman transport between two consecutive surveys
$\bar{R}$	Average river water flux between two consecutive surveys
$\frac{\Delta S/\Delta t, \Delta T/\Delta t}{\bar{R} \times \bar{T}_R}$	Changes in the salt and heat (temperature) content of the system between two consecutive surveys Average river heat (temperature) flux between two consecutive surveys
$\frac{\bar{S}_B, \bar{S}_S}{\bar{T}_B, \bar{T}_S}$	Average bottom and surface salinity at the boundaries of the system between two consecutive surveys Average bottom and surface temperature at the boundaries of the system between two consecutive surveys
$V$	Study volume of the Ría de Vigo
$\bar{w}$	Weighting factor of the relative contribution of salinity and temperature to the density gradient
$\bar{W}$	Average sewage water flux ( $0.5 \text{ m}^3 \text{ s}^{-1}$ ) between two consecutive surveys

$\mu\text{mol C L}^{-1}$  ( $n = 44$ ) for the blank reference material. The nominal values provided by the reference laboratories are  $44.0 \pm 1.5$  and  $0.0 \pm 1.5 \mu\text{mol C L}^{-1}$ , respectively.

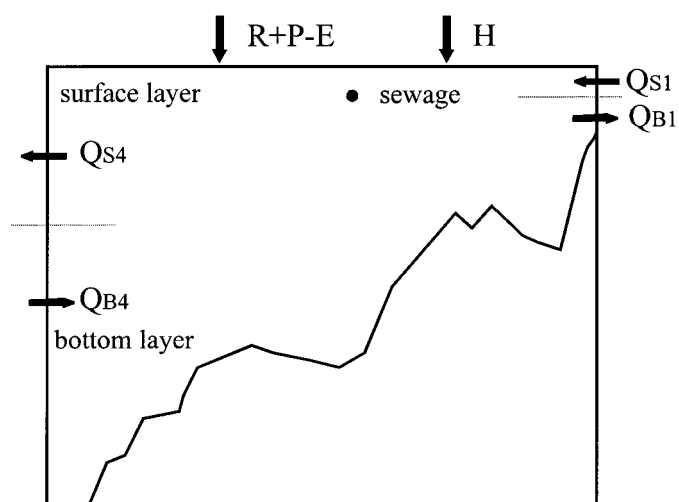


Fig. 2. Section across the central channel of the Ría de Vigo showing the study system—with surface and bottom layer—delimited by the inner (1) and outer (4) boundaries (Fig. 1).  $R + P - E$ , hydrological balance (continental runoff + precipitation – evaporation).  $H$ , heat exchange across the sea surface.  $Q_{B1}$  and  $Q_{B4}$ , bottom horizontal advective fluxes at the inner and outer boundary.  $Q_{S1}$  and  $Q_{S4}$ , surface horizontal advective fluxes at the inner and outer boundary. Sewage, advective flux from the sewage of the city of Vigo.

*Estimation of the NEP of DOC with a two-dimensional box model*—The transient two-dimensional mass-heat-weighted box model used by Rosón et al. (1997) in the adjacent Ría de Arousa has been adapted to the Ría de Vigo. The box model estimates the average residual exchange fluxes (horizontal and vertical advection and vertical mixing) that produce the salinity and temperature changes observed in the embayment between two consecutive surveys, separated by 2–4 d. For the purposes of this work, only the horizontal advective fluxes will be considered. Table 1 defines the relevant terms of the model used throughout the text.

Two boundaries are defined that delimit the study system (Fig. 2). The inner limit separates the ría from San Simón Bay, the estuary of the river Oitabén-Verdugo. The outer limit separates the ría from the continental shelf off the Rías Baixas. Each boundary consists of two layers (surface and bottom), flowing in opposite directions. The level of no horizontal motion between the surface and bottom layer is the gravity center of the boundary, i.e., the depth at which the actual density coincides with the average density of the boundary (Rosón et al. 1997). The average salinity and temperature of the surface and bottom layer of each boundary and box are obtained by integration of the calibrated CTD profiles. For each boundary we can define the average flux of surface water ( $\bar{Q}_S$ ,  $\text{m}^3 \text{ s}^{-1}$ ), salt ( $\overline{Q_S \times S_S}$ ,  $\text{kg s}^{-1}$ ) and heat

$\overline{Q_s \times T_s}$ ,  $^{\circ}\text{C m}^3 \text{s}^{-1}$ ) between two consecutive surveys. Equations for volume, salt, and heat conservation can be written for the segment delimited within the boundary: San Simón Bay for the case of boundary 1 and the ría + San Simón bay for the case of boundary 4 (Fig. 2).

$$\bar{Q}_s = \bar{Q}_B + \bar{R}, \quad (2)$$

$$V \times \frac{\Delta S}{\Delta t} = \bar{Q}_B \times \bar{S}_B - \bar{Q}_s \times \bar{S}_s, \quad (3)$$

$$V \times \frac{\Delta T}{\Delta t} = \bar{R} \times \bar{T}_R + \bar{H} + \bar{Q}_B \times \bar{T}_B - \bar{Q}_s \times \bar{T}_s, \quad (4)$$

where  $\bar{R}$  ( $\text{m}^3 \text{s}^{-1}$ ) and  $\bar{R} \times \bar{T}_R$  ( $^{\circ}\text{C m}^3 \text{s}^{-1}$ ) are the average water and heat fluxes due to continental runoff between two consecutive surveys.  $\bar{H}$  ( $^{\circ}\text{C m}^3 \text{s}^{-1}$ ) is the average air-sea heat-exchange flux across the sea surface of the segment delimited within the boundary between two consecutive surveys.  $V$  ( $\text{m}^3$ ) is the volume of the segment limited within the boundary.  $\Delta S/\Delta t$  ( $\text{kg m}^{-3} \text{s}^{-1}$ ) and  $\Delta T/\Delta t$  ( $^{\circ}\text{C s}^{-1}$ ) are the average salinity and temperature change on the segment delimited by the boundary between two consecutive surveys.  $\bar{Q}_B$  ( $\text{m}^3 \text{s}^{-1}$ ),  $\bar{Q}_B \times \bar{S}_B$  ( $\text{kg s}^{-1}$ ) and  $\bar{Q}_B \times \bar{T}_B$  ( $^{\circ}\text{C m}^3 \text{s}^{-1}$ ) are the average fluxes of water, salt, and heat in the bottom layer between two consecutive surveys. It should be noticed that  $\bar{R}$ ,  $\bar{H}$ ,  $V$ ,  $\Delta S/\Delta t$ , and  $\Delta T/\Delta t$  refer to the drainage basin, the surface area, and the volume of San Simón Bay for the case of boundary 1 and of the ría + San Simón Bay for the case of boundary 4.

Two reasonable assumptions are implicit in the system of equations: (1) the volume of the ría is constant; and (2) the contribution of the  $P - E$  term to the water budget is negligible. In fact, the  $P - E$  term was calculated to verify its minor contribution. Another less-obvious assumption is that horizontal mixing can be ignored. The horizontal circulation in the ría is controlled by shelf wind stress, which produces enhanced advection. Horizontal velocities are normally  $>3 \times 10^{-2} \text{ m s}^{-1}$ , whereas turbulent diffusion coefficients are  $\sim 10 \text{ m}^2 \text{ s}^{-1}$  (Rosón et al. 1997). Considering these numbers and the observed DOC gradients in the ría (Figs. 3, 5–7), the contribution of horizontal mixing to net DOC fluxes is usually  $<5\%$ .

The extreme variability of water fluxes, compared with salinity and temperature changes between two consecutive surveys allows the simplification of Eqs. (3) and (4):

$$V \times \frac{\Delta S}{\Delta t} = \bar{Q}_B \times \bar{S}_B - \bar{Q}_s \times \bar{S}_s \quad (5)$$

$$V \times \frac{\Delta T}{\Delta t} = \bar{R} \times \bar{T}_R + \bar{H} + \bar{Q}_B \times \bar{T}_B - \bar{Q}_s \times \bar{T}_s. \quad (6)$$

Two sets of water fluxes can be obtained, from the equations of water (1) and salt (5) conservation,  $(\bar{Q}_s)_s$ , and the equations of water (1) and heat (6) conservation,  $(\bar{Q}_s)_T$ :

$$(\bar{Q}_s)_s = \frac{\bar{R} \times \bar{S}_B + V \times \frac{\Delta S}{\Delta t}}{\bar{S}_B - \bar{S}_s}, \quad (7)$$

$$(\bar{Q}_s)_T = \frac{\bar{R} \times (\bar{T}_B - \bar{T}_R) - \bar{H} + V \times \frac{\Delta T}{\Delta t}}{\bar{T}_B - \bar{T}_s}. \quad (8)$$

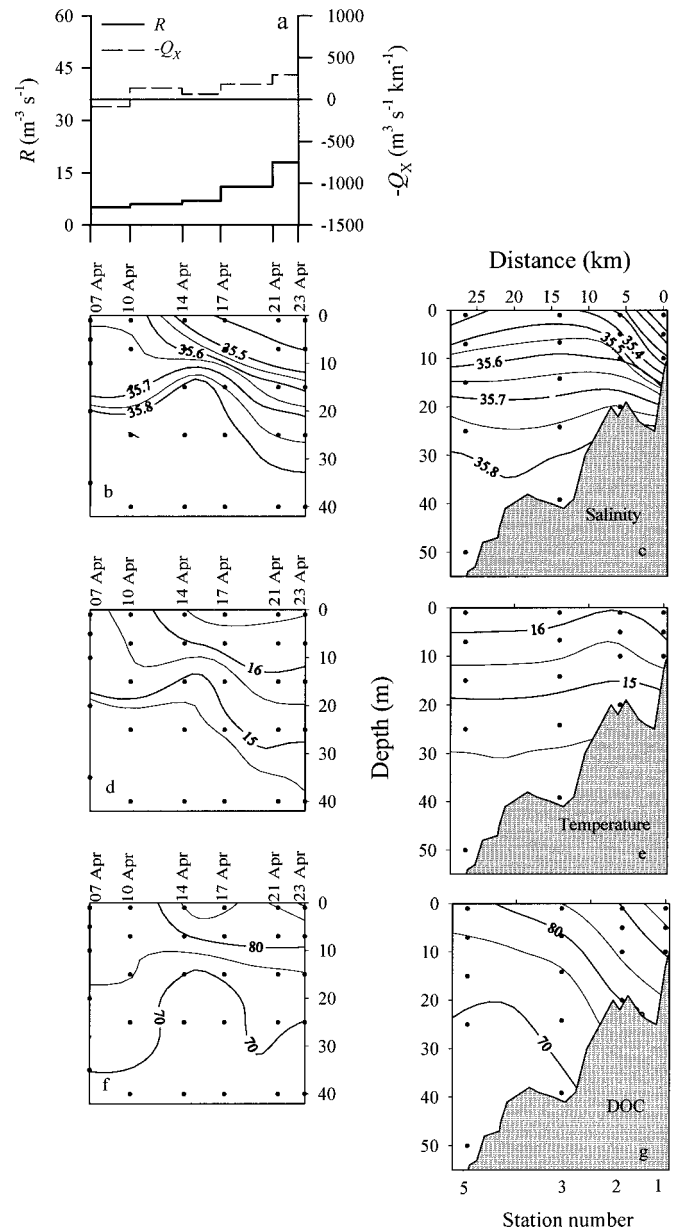


Fig. 3. (a) Time course of continental runoff,  $R$ , and offshore Ekman transport,  $-Q_x$ , (b) salinity, (d) temperature, and (f) DOC profiles at Sta. 3. (c) Average salinity, (e) temperature, and (g) DOC profiles along the central axis of the Ría de Vigo during the first sampling period: 7–23 April 1997.  $R$  in  $\text{m}^3 \text{s}^{-1}$ ,  $-Q_x$  in  $\text{m}^3 \text{s}^{-1} \text{km}^{-1}$ , salinity in pss, temperature in  $^{\circ}\text{C}$ , and DOC in  $\mu\text{mol C L}^{-1}$ .

Finally, the mass-heat-weighted water flux,  $\bar{Q}_s$ , is estimated as

$$\bar{Q}_s = (\bar{Q}_s)_s \times (1 - \bar{w}) + (\bar{Q}_s)_T \times \bar{w}, \quad (9)$$

where  $\bar{w}$  is a dimensionless factor that weights the contribution of salinity and temperature to the density gradient, the responsible of the observed water fluxes:

$$\bar{w} = \frac{(\bar{T}_B - \bar{T}_s)^2}{(\bar{T}_B - \bar{T}_s)^2 + \left(\frac{\beta}{\alpha}\right)^2 (\bar{S}_B - \bar{S}_s)^2}. \quad (10)$$

The ratio of the coefficients of haline contraction and thermal expansion,  $\bar{\beta}/\bar{\alpha}$ , is used to convert the salinity gradient into temperature units:

$$\frac{\bar{\beta}}{\bar{\alpha}} = \frac{\frac{1}{\rho} \times \left( \frac{\partial \rho}{\partial S} \right)_T}{-\frac{1}{\rho} \times \left( \frac{\partial \rho}{\partial T} \right)_S} \quad (11)$$

$\bar{\beta}/\bar{\alpha}$  was calculated from the equation of state of seawater (UNESCO 1985) for the average salinity and temperature of each boundary between  $t_1$  and  $t_2$ .

Once water fluxes are known, the average budget of DOC outputs minus inputs ( $O - I$ , mol C s<sup>-1</sup>) between two consecutive surveys can be calculated as

$$\begin{aligned} O - I &= \bar{Q}_S \times \overline{\text{DOC}}_S - (\bar{Q}_S - \bar{R}) \times \overline{\text{DOC}}_B \\ &\quad - \bar{R} \times \overline{\text{DOC}}_R - \bar{W} \times \overline{\text{DOC}}_W \\ &= \bar{Q}_S \times (\overline{\text{DOC}}_S - \overline{\text{DOC}}_B) \\ &\quad - \bar{R} \times (\overline{\text{DOC}}_R - \overline{\text{DOC}}_B) - \bar{W} \times \overline{\text{DOC}}_W, \end{aligned} \quad (12)$$

where  $\text{DOC}_S$  and  $\text{DOC}_B$  are the average concentration of DOC in the surface and bottom horizontal fluxes and  $\bar{W}$  and  $\text{DOC}_W$  are the average flux of water and the concentration of DOC in the sewage from the city of Vigo (Fig. 1).  $\text{DOC}_R$  and  $\text{DOC}_W$  are set to 400 and  $3.6 \times 10^3 \mu\text{mol C L}^{-1}$ , respectively (Doval et al. 1997).

Finally, the average net ecosystem production of DOC, NEP, in the study system is

$$\overline{\text{NEP}} = V \times \frac{\Delta \text{DOC}}{\Delta t} + O - I. \quad (13)$$

The box-model approach might involve large potential errors in the estimation of the NEP of DOC, but it is a unique method to measure the whole community metabolism directly (Smith and Hollibaugh 1997) and avoids most of the problems associated with *in vitro* methods: reduced turbulence, unnatural light fields, and altered grazer communities. Therefore, box-model estimations of rate measurements are probably less accurate than *in vitro* techniques, but the resulting values are ready for direct interpretation at the ecosystem level.

## Results

The Ría de Vigo was intensively sampled during four distinct periods during 1997, looking for contrasting hydrodynamic (upwelling and downwelling) and biogeochemical (ecosystem production and respiration of DOC) conditions. The short time and space variability of the salinity, temperature, and DOC profiles and the corresponding outputs from the two-dimensional box model (water and DOC fluxes and net DOC production and accumulation) are presented for each period. The results are appraised on the light of the response to the external forces acting on the embayment (continental runoff, offshore Ekman transport).

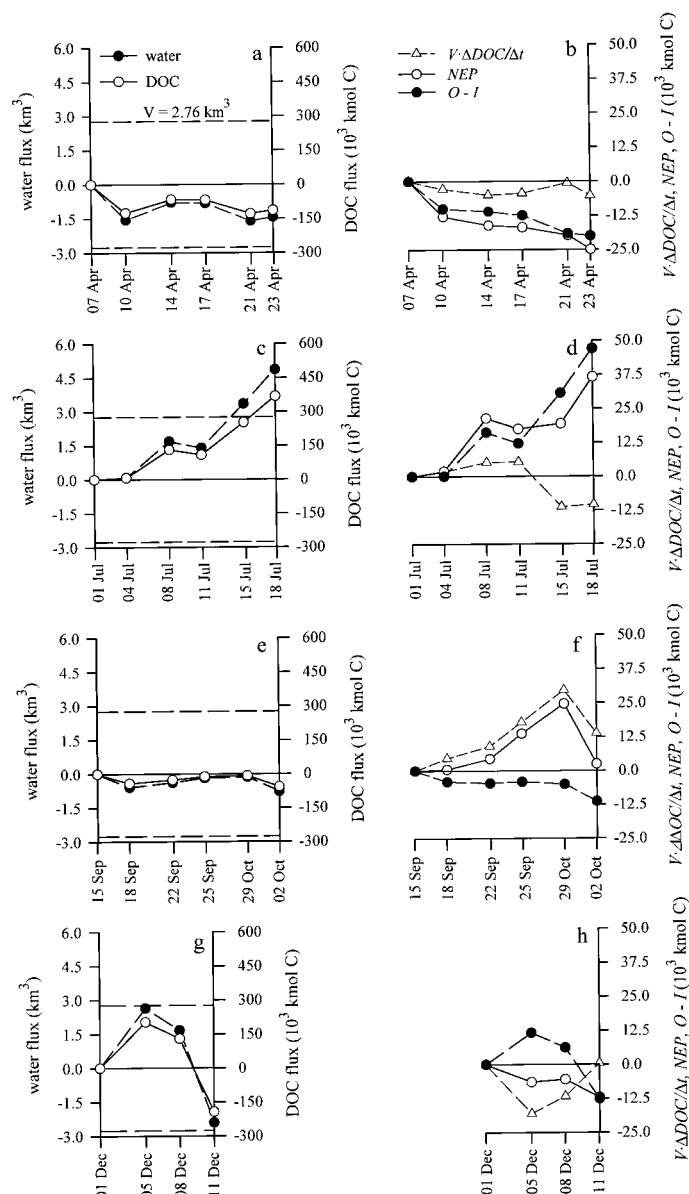


Fig. 4. Time course of cumulative water flows and DOC surface fluxes in the outer boundary of the ría during the (a) first sampling period: 7–23 April 1997, (c) second sampling period: 1–18 July 1997, (e) third sampling period: 15 September–2 October 1997; and (g) fourth sampling period: 1–11 December 1997. Also included are time course of the net  $O - I$  balance, the accumulation term ( $V \times \Delta \text{DOC}/\Delta t$ ) and NEP in the system during the (b) first sampling period: 7–23 April 1997, (d) second sampling period: 1–18 July 1997, (f), third sampling period: 15 September–2 October 1997, and (h) fourth sampling period: 1–11 December 1997. To convert kmol C into mmol C m<sup>-2</sup> d<sup>-1</sup>, multiply by  $8.55 \times 10^{-3}/\Delta t$ , where  $\Delta t$  is the corresponding time interval in days.

*Spring: consumption of DOC imported from the shelf during downwelling*—Shelf winds were moderate in intensity and variable in direction during the spring survey, producing offshore Ekman transport absolute values  $<300 \text{ m}^3 \text{ s}^{-1} \text{ km}^{-1}$  (Fig. 3a). Continental runoff was rather low, increasing from

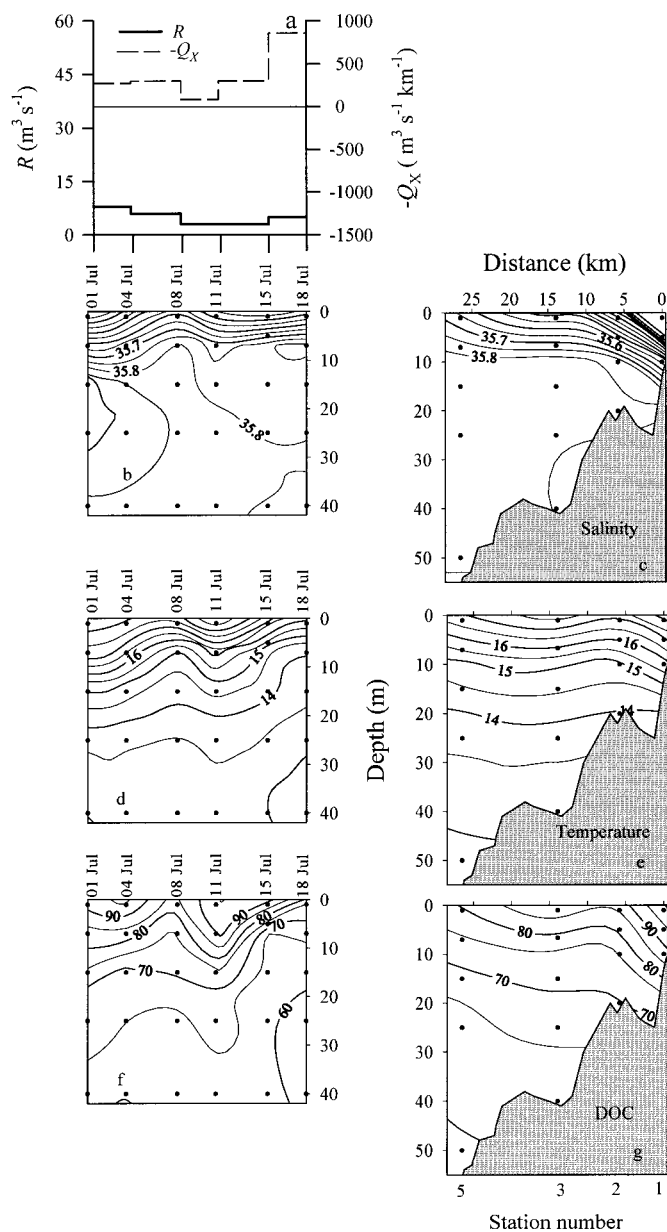


Fig. 5. (a) Time course of continental runoff,  $R$ , and offshore Ekman transport,  $-Q_x$ , (b) salinity, (d) temperature, and (f) DOC profiles at Sta. 3. (c) Average salinity, (e) temperature, and (g) DOC profiles along the central axes of the Ría de Vigo during the second sampling period: 1–18 July 1997.  $R$  in  $\text{m}^3 \text{s}^{-1}$ ,  $-Q_x$  in  $\text{m}^3 \text{s}^{-1} \text{km}^{-1}$ , salinity in pss, temperature in  $^{\circ}\text{C}$ , and DOC in  $\mu\text{mol C L}^{-1}$ .

4 to  $17 \text{ m}^3 \text{ s}^{-1}$ . Since the surface layer of the outer boundary of the Ría de Vigo is  $\sim 10 \text{ km}$  wide, the relative contribution of the offshore Ekman transport to water circulation in the embayment was  $\sim 2$  orders of magnitude larger than the contribution of continental runoff.

The short-timescale evolution of the salinity (Fig. 3b) and temperature (Fig. 3d) profiles in the middle Ría de Vigo (Sta. 3) reacted to the observed meteorological variability. The evolution of the  $35.8 \text{ pss}$  and  $15^{\circ}\text{C}$  isolines were parallel, showing a net entry of eastern North Atlantic Central Water

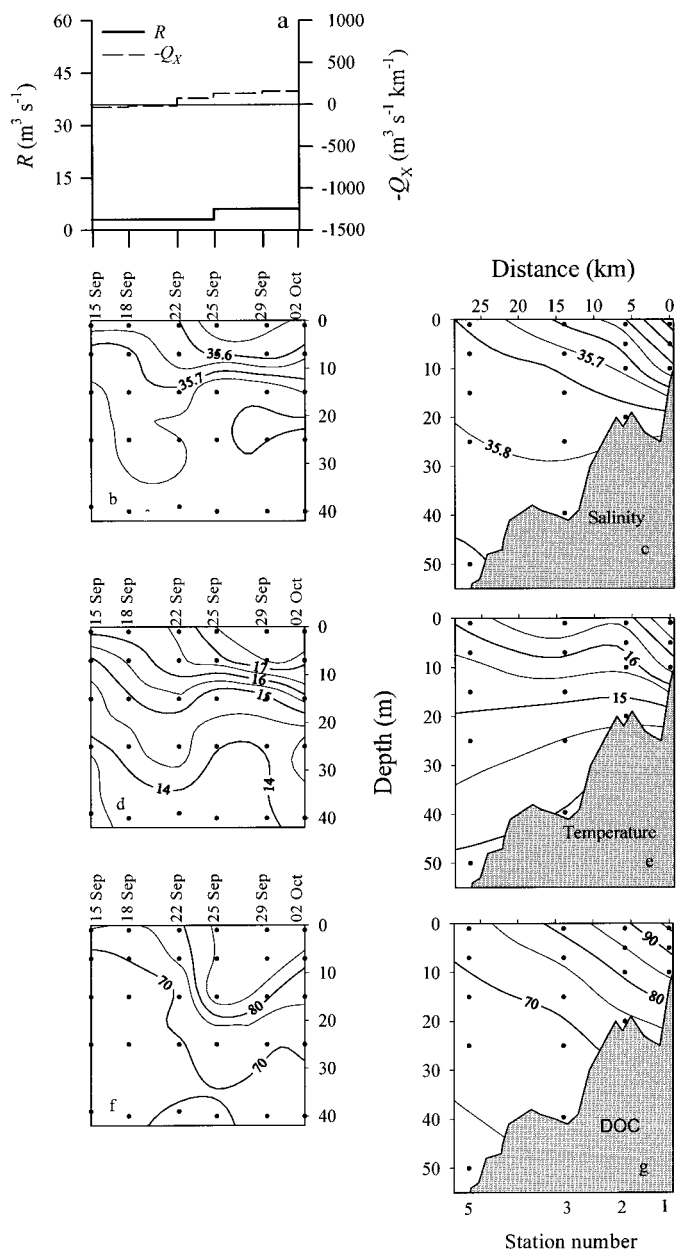


Fig. 6. (a) Time course of continental runoff,  $R$ , and offshore Ekman transport,  $-Q_x$ , (b) salinity, (d) temperature, and (f) DOC profiles at Sta. 3. (c) Average salinity, (e) temperature, and (g) DOC profiles along the central axes of the Ría de Vigo during the third sampling period: 15 September–2 October 1997.  $R$  in  $\text{m}^3 \text{ s}^{-1}$ ,  $-Q_x$  in  $\text{m}^3 \text{ s}^{-1} \text{ km}^{-1}$ , salinity in pss, temperature in  $^{\circ}\text{C}$ , and DOC in  $\mu\text{mol C L}^{-1}$ .

(ENACW) from the bottom shelf between 10 and 14 April that corresponds with a brief upwelling-favorable wind peak. Subsequent wind relaxation was accompanied by dramatic withdraw of ENACW from 17 to 21 April, which was partially restored by upwelling-favorable winds at the end of the period (21–23 April). Salinity decreased and temperature increased in the surface layer along the period. The time evolution of DOC (Fig. 3f) was parallel to salinity and temperature. The  $70\text{-}\mu\text{mol C L}^{-1}$  isoline resembled ENACW

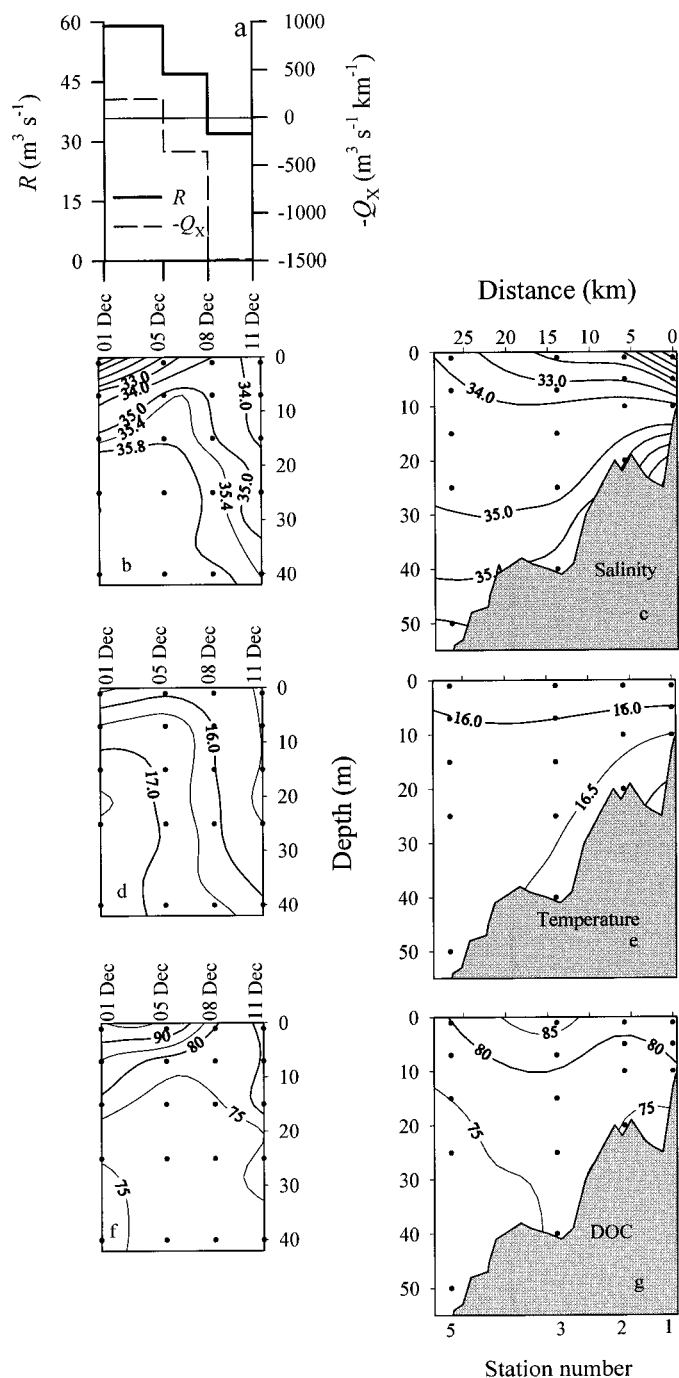


Fig. 7. (a) Time course of continental runoff,  $R$ , and offshore Ekman transport,  $-Q_x$ , (b) salinity, (d) temperature, and (f) DOC profiles at Sta. 3. (c) Average salinity, (e) temperature, and (g) DOC profiles along the central axes of the Ría de Vigo during the fourth sampling period: 1–11 December 1997.  $R$  in  $\text{m}^3 \text{s}^{-1}$ ,  $-Q_x$  in  $\text{m}^3 \text{s}^{-1} \text{km}^{-1}$ , salinity in pss, temperature in  $^{\circ}\text{C}$ , and DOC in  $\mu\text{mol C L}^{-1}$ .

displacements inferred above. In the surface layer, increasing stratification from 14 April was accompanied by DOC accumulation.

The 7–23 April average salinity (Fig. 3c), temperature (Fig. 3e), and DOC (Fig. 3g) profiles along the main channel

of the inlet illustrate marked spatial differences, which fitted with relative location in regard to the external forces: runoff in the inner boundary and Ekman transport in the outer boundary. It is worth noting the wide DOC range, from  $<70 \mu\text{mol C L}^{-1}$  in upwelled ENACW colder than  $14^{\circ}\text{C}$  to  $>95 \mu\text{mol C L}^{-1}$  in DOC outwelled from San Simón Bay.

Figure 4a shows the cumulative surface water flux at the outer boundary of the ría, obtained with the two-dimensional box model. Despite the outgoing direction of the flux from 10 to 14 and 21 to 23 April, the ría imported  $1.42 \text{ km}^3$  of shelf surface waters during the whole period (Table 2),  $\sim 51\%$  of its volume ( $2.76 \text{ km}^3$ ). On the other hand,  $0.80 \text{ km}^3$  of San Simón Bay water were introduced in the surface layer of the ría across the inner boundary. Continental runoff and sewage contributions were negligible. The flushing time of the system was  $\sim 20 \text{ d}$  (renewal rate,  $5\% \text{ d}^{-1}$ ). The DOC surface flux at the outer boundary (Fig. 4a) compasses the water flux, denoting a net entry of  $114.7 \times 10^3 \text{ kmol C}$  (average  $81 \mu\text{mol C L}^{-1}$ ) from shelf surface waters,  $58.2\%$  of the total DOC input (Table 2). San Simón Bay contributed with  $79.6 \times 10^3 \text{ kmol C}$  (average  $100 \mu\text{mol C L}^{-1}$ ),  $40.3\%$  of the total input. Continental runoff and sewage from the city of Vigo were minor DOC donors,  $1.5\%$  of the total input.

The cumulative net balance of DOC outputs minus inputs ( $O - I$ ; Fig. 4b) resembled the DOC surface flux across the outer boundary of the ría (Fig. 4a), yielding a net difference of  $-20.0 \times 10^3 \text{ kmol C}$ , i.e.,  $-10\%$  of the total input. Therefore, during the spring period the ría imported DOC, mainly from shelf surface waters at the outer boundary and San Simón Bay at the inner boundary. The cumulative NEP of DOC parallels the net  $O - I$  balance, demonstrating an in-depth short-timescale (2–4 d) coupling between net DOC import and oxidation. The largest DOC net consumption rates,  $\text{NEP} = -49.8 \text{ mol C s}^{-1}$ , occurred between 7 and 10 April (Table 3), when  $\sim 93\%$  of the DOC that entered the ría came from shelf surface waters accompanying a strong reversal of the positive circulation in the outer boundary. During these 3 d, it oxidized  $\sim 50\%$  of the total amount of DOC consumed along the whole 16-d period. The net  $O - I$  balance represents  $80\%$  of the net ecosystem consumption of DOC in the system ( $\text{NEP} = -25 \times 10^3 \text{ kmol C}$ ). The remaining  $20\%$  came from the DOC previously accumulated in the ría ( $V \times \Delta\text{DOC}/\Delta t = -5 \times 10^3 \text{ kmol C}$ ).

*Summer: export to the shelf of DOC produced during upwelling*—The summer period—in the middle of the upwelling season—coincided with upwelling-favorable northerly winds that produce offshore Ekman transport values ranging between  $85$  and  $860 \text{ m}^3 \text{ s}^{-1} \text{ km}^{-1}$  (Fig. 5a). On the contrary, continental runoff was extremely low:  $<7 \text{ m}^3 \text{ s}^{-1}$ .

The short-timescale evolution of the salinity (Fig. 5b) and temperature (Fig. 5d) profiles indicate water displacements in agreement with shelf-wind forcing (Fig. 5a). Upwelling-favorable winds from 1 to 8 July produced the entry of ENACW that was colder ( $<14^{\circ}\text{C}$ ) and saltier ( $>35.9 \text{ pss}$ ) than that during the spring period. Wind relaxation from 8 to 11 July was accompanied by the corresponding isopleths deepening. Finally, strong upwelling-favorable winds from 11 to 18 July produced the massive entry of ENACW colder than

Table 2. Summary of the cumulative water flows (in km<sup>3</sup>) and DOC fluxes (in 10<sup>3</sup> kmol C) in the surface and bottom, inner and outer boundaries of the Ría de Vigo ( $Q_{S1}$ ,  $Q_{B1}$ ,  $Q_{S4}$ ,  $Q_{B4}$ ), river (R) and sewage discharges during the four study periods. See Fig. 2 for reference.

Survey period			$Q_{S4}$	$Q_{B4}$	$Q_{S1}$	$Q_{B1}$	R	Sewage
Spring	07–23 Apr	Water	−1.42	−1.44	0.80	0.79	$1.1 \times 10^{-3}$	$0.7 \times 10^{-3}$
		DOC	−114.7	−105.2	79.6	72.0	0.45	2.5
Summer	01–18 Jul	Water	4.87	4.86	0.31	0.30	$2.6 \times 10^{-8}$	$0.7 \times 10^{-3}$
		DOC	367.6	312.9	30.9	27.1	1.08	2.64
Autumn	15 Sep–2 Oct	Water	−0.78	−0.78	0.48	0.47	$2.3 \times 10^{-3}$	$0.7 \times 10^{-3}$
		DOC	−57.6	−53.3	44.3	40.8	0.92	2.64
Winter	01–11 Dec	Water	−2.36	−2.42	0.20	0.17	$15.5 \times 10^{-3}$	$0.4 \times 10^{-8}$
		DOC	−193.6	−192.3	17.2	13.7	6.17	1.55

13°C in the middle ría. DOC profiles (Fig. 5f) followed the variability of the thermohaline properties. The 70  $\mu\text{mol C L}^{-1}$  isoline is parallel to the 14°C–15°C isopleths, and DOC concentrations <60  $\mu\text{mol C L}^{-1}$  were recorded for temperatures <13°C. On the other hand, DOC levels >90  $\mu\text{mol C L}^{-1}$  were observed in stratified surface waters during upwelling relaxation. The average effect of upwelling on the salinity (Fig. 5c), temperature (Fig. 5e), and DOC (Fig. 5g) profiles along the main axis of the embayment can be clearly observed. Bottom water saltier than 35.8 pss, colder than 14°C, and with DOC concentration <70  $\mu\text{mol C L}^{-1}$  penetrated up to the shallow reaches of the inner ría.

As a result of the prevailing northerly winds over the shelf, water circulation at both the inner and outer boundaries of the ría was positive (Fig. 4c, Table 2). A volume of 4.86 km<sup>3</sup> of ENACW upwelled over the shelf entered the ría across the bottom outer boundary from 1 to 18 July. On the contrary, only 0.31 km<sup>3</sup> of San Simón Bay water entered across the surface inner boundary. The contributions of continental runoff and sewage were again negligible. The flushing time of the system during this period reduced to only 9 d (renewal rate, 11% d<sup>−1</sup>), and the exchange across the outer boundary accounted for 94% of the total renewal. The circulation was particularly intensified from 11 to 18 July. In agreement with the circulation pattern, the main DOC source to the ría was the DOC-poor ENACW (average 64  $\mu\text{mol C L}^{-1}$ ) that represented 90.0% of the total DOC influx. DOC entering the ría from San Simón Bay (average 100  $\mu\text{mol C L}^{-1}$ ) amounted 8.9% of the total input (Table 2).

The cumulative  $O - I$  balance of DOC (Fig. 4d) yields a net difference of  $+47.1 \times 10^3$  kmol C, revealing that the ría was acting as a DOC source to shelf surface waters. The cumulative NEP of DOC is coupled with the net  $O - I$  balance that, in turn, goes with the surface water flow in the outer boundary (Fig. 4a). The DOC produced within the ría at the timescale of the flushing time ( $\tau = 9$  d) represented ~80% of the total amount of DOC exported to the shelf. The exported material was produced during the vigorous upwelling episodes of 4–8 and 15–18 July, when the NEP of DOC was 56.5 and 66.5 mol C s<sup>−1</sup>, respectively (average 60.9 mol C s<sup>−1</sup>; Table 3). The final 20% of DOC exported to the shelf came from materials previously accumulated in the ría and involved a 5% reduction of the DOC amount in the ría at the beginning of the period.

*Autumn: in situ production and consumption of DOC during wind relaxation*—A prolonged (>10-d) wind calm—characteristic of the transition from the upwelling- to the downwelling-favorable season (Nogueira et al. 1997)—was monitored during this period. The offshore Ekman transport ranged from −30 to 160 m<sup>3</sup> s<sup>−1</sup> km<sup>−1</sup> (Fig. 6a). Continental runoff was also quite limited: <5 m<sup>3</sup> s<sup>−1</sup>. Under these conditions, the time evolution of the salinity (Fig. 6b), temperature (Fig. 6d), and DOC (Fig. 6f) profiles indicate a broad trend to withdraw the salty, cold, and DOC-poor ENACW in the bottom layer of the middle ría. However, from 18 to 28 September the 14°C isobath pointed to a transitory re-entry of ENACW into the ría. In the surface layer, stratifi-

Table 3. Summary of the DOC standing stocks ( $\mu\text{mol C L}^{-1}$ ),  $O - I$  and NEP rates (mol C s<sup>−1</sup>), and DOC turnover times (% d<sup>−1</sup>) for the spring, summer, autumn, and winter surveys. Average values for the selected time intervals described in the text for each period. The turnover time of the entire DOC pool has been calculated as  $\text{NEP} \times 86,400 \times 100 / (\text{DOC} \times 2.76 \times 10^6)$ . To convert mol C s<sup>−1</sup> into mmol C m<sup>−2</sup> d<sup>−1</sup>, values in mol C s<sup>−1</sup> have to be multiplied by  $1000 \times 86,400 / (117 \times 10^6)$ . Volume of the ría:  $2.76 \times 10^9$  m<sup>3</sup>, surface of the ría  $117 \times 10^6$  m<sup>2</sup>.

Survey period		DOC	$O - I$	NEP	Turnover time
Spring	07–10 Apr	77	−38.9	−49.8	−2.0
	10–23 Apr	76	−8.8	−11.1	−0.5
Summer	01–04/08–15 Jul	72	+16.8	−0.1	−0.0
	04–08/15–18 Jul	71	+53.8	+60.9	+2.7
Autumn	15–29 Sep	73	−4.2	+20.3	+0.9
	29 Sep–02 Oct	76	+24.4	−85.6	−3.6
Winter	01–05 Dec	77	+33.7	−18.6	−0.8
	05–11 Dec	76	−46.8	−10.9	−0.4

cation increased with time, and it was accompanied by a marked accumulation of DOC ( $>85 \mu\text{mol C L}^{-1}$ ). The average salinity (Fig. 6c), temperature (Fig. 6e), and DOC (Fig. 6g) distributions along the main axis of the ría show limited haline and strong temperature and DOC gradients, similar to the observations made during the spring period (Fig. 3c,e,g).

Prolonged wind relaxation produced limited water exchange across the outer boundary of the ría through this period (Fig. 4e, Table 2). Only 17% and 28% of the volume of the ría was renewed with San Simón Bay and continental shelf surface waters, respectively. Therefore, the flushing time was extremely large: 38 d (renewal rate,  $2.6\% \text{ d}^{-1}$ ). Accordingly, DOC exchange fluxes were very limited, compared with the spring and summer periods. Only  $57.6 \times 10^3 \text{ kmol C}$  entered from shelf surface waters (average  $74 \mu\text{mol C L}^{-1}$ ) and  $44.3 \times 10^3 \text{ kmol C}$  from San Simón Bay (average  $92 \mu\text{mol C L}^{-1}$ ). Continental runoff and sewage represented 0.9% and 2.5% of the total DOC input to the ría (Table 2).

Progressive accumulation of the DOC produced from 15 to 29 September, at an average NEP rate of  $+20.3 \text{ mol C s}^{-1}$ , was observed (Fig. 4f; Table 3). By 29 September, the NEP of DOC amounted  $+24.6 \times 10^3 \text{ kmol C}$ , which represents 83% of the total DOC accumulation. It is interesting to note that, during these 11 d, a slow-moving positive circulation was restored, producing a net entry of  $0.45 \text{ km}^3$  of DOC-poor ENACW from the bottom shelf. DOC produced during this third period was not exported as in the summer period but accumulated into the ría. The remaining 17% of accumulated DOC came from the net import of extrinsic materials, accounted by the  $O - I$  balance. The close coupling between the surface water and DOC fluxes at the outer boundary and the  $O - I$  balance suggests that most of the external DOC accumulated in the system came from the shelf. The initial DOC amount in the ría at the beginning of the study period ( $188.4 \times 10^3 \text{ kmol C}$ ) increased by +16% on 29 September. However, during the subsequent reversal of the circulation pattern from 29 September to 2 October,  $\sim 90\%$  of the DOC produced during the previous days was consumed at the extremely high net rate of  $85.6 \text{ mol C s}^{-1}$  (Table 3).

*Winter: exchange and accumulation of DOC during the unproductive season*—Dramatic changes occurred during this period in the wind regime (Fig. 7a), evolving from upwelling favourable northerly winds on 1–5 December ( $200 \text{ m}^3 \text{ s}^{-1} \text{ km}^{-1}$ ) to downwelling-favorable southerly winds on 8–11 December ( $-1500 \text{ m}^3 \text{ s}^{-1} \text{ km}^{-1}$ ). Continental runoff was high, ranging from  $52 \text{ m}^3 \text{ s}^{-1}$  on 1–5 December to  $26 \text{ m}^3 \text{ s}^{-1}$  on 8–11 December.

Time changes in the salinity (Fig. 7b), temperature (Fig. 7d), and DOC (Fig. 7f) profiles are concomitant with the wind regime, showing dramatic changes in the orientation of the isopleths (see  $35.0 \text{ pss}$ ,  $17.0 \text{ }^\circ\text{C}$ , and  $75 \mu\text{mol C L}^{-1}$  for reference). Despite the winter conditions, bottom waters of the ría were warm and salty, as expected in the Iberian upwelling system at this time of the year. A poleward-flowing slope current of warm and salty subtropical water is usually observed (Haynes and Barton 1990). Under strong downwelling conditions, these subtropical waters enter the rías, as occurs from 5 to 11 December. Downwelling was so

intense that water column homogenisation in the middle ría was almost complete. This contrast with the situation observed from 1 to 5 December, when the positive circulation pattern accompanying the initial upwelling displaced the fresh and DOC-rich water from San Simón Bay to the middle ría (Sta. 3). The average distributions along the main axis show the westward extension of the fresh (Fig. 7c) and DOC-rich (Fig. 7g) water outwelled from San Simón Bay and the thermal homogenization (Fig. 7e) accompanying the entry of warm subtropical surface waters from the shelf.

Intense positive circulation occurred at the outer boundary of the ría at the beginning of this period (Fig. 4g). Water exchange with the adjacent shelf, at the extremely high average rate of  $7.6 \times 10^3 \text{ m}^3 \text{ s}^{-1}$  from 1 to 5 December, equalled the whole volume of the ría. However, from 5 to 11 December, a dramatic reversal of the circulation pattern accompanied the dominant downwelling-favorable southerly winds. As much as  $5.50 \text{ km}^3$  entered the ría across the surface outer boundary, reintroducing twice the volume exported during the initial upwelling episode. Consequently, for the whole period, the ría imported  $2.36 \text{ km}^3$  of shelf surface water (Table 2), i.e., 86% of its volume. The flushing time during this period was 11 days (renewal rate,  $9\% \text{ d}^{-1}$ ). DOC fluxes followed the circulation pattern (Fig. 4g, Table 2), with  $193.6 \times 10^3 \text{ kmol C}$  (average  $82 \mu\text{mol L}^{-1}$ ) entering the surface outer boundary (88.6%) and  $17.2 \times 10^3 \text{ kmol C}$  (average  $85 \mu\text{mol L}^{-1}$ ) entering the surface inner boundary (7.9%). Continental runoff and sewage represented 2.8% and 0.7% of the total DOC input, respectively.

The  $O - I$  balance of DOC (Fig. 4h) was again parallel to the water and DOC fluxes across the surface outer boundary, in such a way that  $11.7 \times 10^3 \text{ kmol C}$  of DOC were exported to the shelf between 1 and 5 December, whereas  $24.3 \times 10^3 \text{ kmol C}$  were imported from 5 to 11 December (Table 3). short-timescale changes in the accumulation term ( $V \times \Delta\text{DOC}/\Delta t$ ) were opposite to the  $O - I$  balance. Export to the shelf during the initial upwelling episode reduced the DOC content of the ría and import during the subsequent downwelling episode restored the previous deficit. The total reduction of the DOC content of the ría from 1 to 5 December was due to export (64%) and oxidation (36%) at an average NEP of  $-18.6 \text{ mol C s}^{-1}$  (Table 3). On the other hand, 23% of the DOC imported from shelf surface waters between 5 and 11 December was oxidized at an average NEP of  $-10.9 \text{ mol C s}^{-1}$ , and 77% accumulated into the ría. It is worth noting that the net DOC-consumption rates by the community of organisms within the ría were much lower than those during the spring downwelling episode (NEP =  $-49.8 \text{ mol C s}^{-1}$ ). As a consequence, the  $O - I$  balance of DOC was coupled with the oxidation term (NEP) during the spring and with the accumulation term ( $V \times \Delta\text{DOC}/\Delta t$ ) during the winter.

## Discussion and conclusions

The four contrasting survey periods present exemplar hydrographic and biogeochemical situations for the northwestern Iberian Peninsula, the northern boundary of the coastal upwelling system that associates to the Canary Current (Bak-

un and Nelson 1991). The Iberian margin system has similarities with the other three major eastern boundary current regions of the world ocean—California, Benguela, and Perú/Humboldt—at comparable latitudes: off Oregon, Republic of South Africa, and Chile, respectively. The study site allowed us to learn about DOC cycling in a coastal upwelling area within an easily accessible coastal inlet in which exchange fluxes can be readily approached and the sampling program is not disturbed by stormy wind conditions.

*Quality of DOC produced/consumed by the community of organisms*—The spring situation illustrates the rapid consumption—at the timescale of the sampling frequency (2–4 d)—of the DOC imported by the system under downwelling conditions. From 7 to 10 April, imported DOC is consumed at the high average net rate of  $-0.37 \text{ mmol C m}^{-2} \text{ d}^{-1}$ . Considering the flushing time for this short event ( $\sim 5$  days), the consumed material has to be judged as labile DOC. Although this material represents a minor ( $\sim 8\%$ ) fraction of the total amount of DOC imported by the ría, it fuels the intense bacterial activity associated to the estimated net consumption rate.

Labile DOC was probably formed in the ría and exported to the shelf during an upwelling episode on the previous days (offshore Ekman transport  $+0.5 \times 10^3 \text{ m}^3 \text{ s}^{-1} \text{ km}^{-1}$  for 3–6 April) and reintroduced into the embayment during the 7–10 April downwelling event. Mid-February to early April is a time of intense net primary production in the study area because of the concurrency of the onset of both the spring bloom and the upwelling-favorable season (Nogueira et al. 1997). Intense net primary production enhances microbial production (exudation and grazing) of labile DOC (Norrman et al. 1995), which can be subsequently consumed by bacteria under favorable conditions for their growth. Downwelling episodes, when the nitracline deepens well below the 1% of photosynthetically active radiation, seem to favor the succession from net production to net respiration regimes in coastal upwelling areas (Pérez et al. 2000). Nutrient depletion affects both phytoplankton and bacterial net growth (Thingstad et al. 1997), but the excess of labile DOC activates bacterial respiration. In fact, the efficiency of conversion of labile DOC into bacterial biomass reduced from 30%–50% in nutrient-rich to  $<5\%$  in nutrient-limited systems (Kirchman et al. 1991; Fuhrman 1992).

In contrast to the spring survey, the summer situation typifies the extensive production of labile DOC under the phytoplankton-dominated regime characteristic of upwelling conditions. Net DOC production exceeded  $+42 \text{ mmol C m}^{-2} \text{ d}^{-1}$  during the intense upwelling episodes of 4–8 and 15–18 July. Average flushing times in the system for these episodes were  $<7$  d. Average net primary production in the ría during the April–October upwelling season is  $100\text{--}125 \text{ mmol C m}^{-2} \text{ d}^{-1}$ . It increases to  $>250 \text{ mmol C m}^{-2} \text{ d}^{-1}$  during upwelling episodes, during which the nitrate-rich ENACW is promoted to surface waters (Moncoiffé et al. 2000). Primary production rates are similar in other coastal upwelling systems of the world ocean (Wollast 1993). Therefore, it is expected that  $\sim 20\%$  of the net primary production in the ría transforms into exportable DOC under upwelling conditions. This percentage is within the 10%–40% range observed in the

equatorial Pacific and other eutrophic systems (Hansell and Carlson 1998). For comparison, these authors obtain percentages of 59%–70% during the spring bloom in the oligotrophic Sargasso Sea. Our percentage is also within the range of much DOC excretion for phytoplankton in coastal areas, 0%–30% (Norrman et al. 1995).

The sustained DOC production of  $+15 \text{ mmol C m}^{-2} \text{ d}^{-1}$  from 15 to 29 September was associated with slow positive circulation provoked by weak coastal upwelling. Such circulation pattern has to produce the gentle injection of nutrients into the surface layer of the ría that supports the primary production rates responsible for the estimated DOC production. The observed thermal stratification, shallow mixed layer, and limited nutrient input through weak upwelling are all favorable to the onset of red-tide assemblages (Cullen et al. 1982; Chang and Carpenter 1985). In fact, red tides used to occur in the Iberian upwelling system at the end of the upwelling season (Figueiras and Ríos 1993), in response to increased stratification, as in other upwelling regions (Barber and Smith 1981). The flushing time in the period 18–29 September is as high as 2 months, which causes the rapid accumulation of the produced DOC. The lability of the accumulated material is confirmed by the extensive consumption of this pool during the reversal of the circulation occurred from 29 September to 2 October. The change in the circulation pattern causes the sudden succession from phytoplankton- to bacteria-dominated regimes and the accumulated labile DOC was consumed at the extremely high net rate of  $-63 \text{ mmol C m}^{-2} \text{ d}^{-1}$ . This net consumption rate is almost twice the rate observed during the spring survey. Lability of the materials and/or bacterial activity can be the causes behind the difference. In this sense, surface temperatures were  $<15.5^\circ\text{C}$  in the spring episode and  $>17.5^\circ\text{C}$  in the autumn episode.

Most of the DOC exchange between the ría and the adjacent shelf during the winter survey is coupled with the accumulation term ( $V \times \Delta\text{DOC}/\Delta t$ ). This is in clear contrast with the coupling between production and export during upwelling episodes (summer) and between respiration and import during downwelling episodes (spring). DOC exchanged across the outer boundary of the ría has recycling times longer than the average 1–11 December flushing time in the study volume (11 d), and must be considered semilabile. Net DOC respiration rates during this period were  $<14 \text{ mmol C m}^{-2} \text{ d}^{-1}$ , i.e.,  $<1/3$  of the rate recorded during the consumption of imported labile DOC during spring. Limited production of labile materials seems to be the reason behind these low respiration rates. The average 1987–1993 December–February nitrate in the surface waters of the ría is  $\sim 7 \mu\text{mol N L}^{-1}$ , and chlorophyll is  $<1 \text{ mg m}^{-3}$  (Nogueira et al. 1997), which indicates reduced net primary production rates. Malfunctioning of the microbial loop by nutrient limitation (Thingstad et al. 1997) can be discarded in this case. In addition, it must be highlighted that cold surface waters are not the reason behind the low bacterial activity, since surface temperature during the winter survey was about the same than during the spring period. As indicated before, this is due to the entry in the ría of warm surface waters transported from subtropical latitudes by the recurrent poleward slope current observed during the winter months. This circulation

pattern is also common in the other three major upwelling systems during the corresponding winter period (Bakun and Nelson 1991).

Smith and Hollibaugh (1997) studied the net ecosystem metabolism of Tomales Bay, a very small ( $8.4 \times 10^{-2} \text{ km}^3$ ) and shallow (3-m deep) well-mixed estuary in the upwelling region of California, which exchanges water slowly with the adjacent shelf (flushing time,  $\sim 3 \text{ wk}$ ). For the case of DOC, they observed insignificant NEP rates either in the summer (maximum offshore Ekman transport) or winter (offshore Ekman transport near zero). Whereas Tomales Bay is a very particular ecosystem within the Californian upwelling, the Ría de Vigo contains a large volume of shelf waters ( $2.76 \text{ km}^3$ , mean depth 20 m, flushing time  $\sim 1 \text{ wk}$ ) representative for carbon cycling in the whole Iberian upwelling system. Therefore, our results are likely representative for the other major upwelling systems of the world ocean.

*Accumulation versus export: hydrodynamic control of the NEP of DOC*—Equation (13) in the “Materials and Methods” section express numerically the possible fate of the NEP of labile DOC in the study ecosystem: (1) increase the DOC standing stock, to make this labile material available to bacterial populations into the system; and/or (2) export out of the ecosystem where the labile material was generated, to serve as new substrate for bacteria in adjacent ecosystems. The ecological implications of the two alternatives are antagonistic, and they are connected to the key issue of regenerated and new production in marine systems (Eppley and Peterson 1979).

The term “NEP” has been throughoutly used in the literature as a synonymous with “new” and “export” production (Quiñones and Platt 1989; Hansell and Carlson 1998). Strictly speaking, NEP and new production have the same meaning: the fraction of the total production supported by nutrients entering from the boundaries of the study ecosystem. However, NEP and export production are equal only under steady-state conditions, i.e., when NEP did not contribute to modify DOC standing stocks in the study volume. The steady-state assumption is operative when appropriately large space ( $>10^{2-3} \text{ km}$ ) and time ( $>10^{2-3} \text{ d}$ ) scales are considered, as in the case of global annual estimates (Walsh 1991; Wollast 1993; Hansell and Carlson 1998). However, at the short time and space scales of the present study the steady-state assumption can lead to severe misinterpretation of the ecosystem functioning.

For steady-state conditions,  $V \times \Delta\text{DOC}/\Delta t = 0$  and  $\text{NEP} = O - I$ . Therefore, the error associated to the steady-state assumption does not affect the qualitative interpretation of the results during the spring (Fig. 4b) and summer (Fig. 4d) surveys because of the close coupling between hydrodynamics (solid dots) and biogeochemistry (open dots) at the short timescale. This is the expected response when the biologically driven recycling time of the materials produced or consumed are shorter than the hydrodynamically driven flushing time of the study volume. Therefore, export to the adjacent ocean is the major fate of labile DOC produced under the very active wind-driven circulation pattern during summer in the Iberian margin (Haynes et al. 1993) and other coastal

upwelling systems (Barber and Smith 1981; Bakun and Nelson 1991).

However, during the autumn (Fig. 4f) and winter (Fig. 4h) surveys, the steady-state assumption would lead to erroneous interpretations. Consideration that the  $O - I$  balance expresses NEP on the study system during the autumn survey would indicate reduced biological activity in response to limited circulation during a period of wind relaxation. However, as much as  $+9 \mu\text{mol C L}^{-1}$  of labile DOC accumulated in the study volume during the initial 11 d and bacteria subsequently consumed them in the final 3 d. Therefore, the autumn situation is a good example of how high NEP at the expense of the nutrient stock accumulated in the ría is not necessarily synonymous with high export. Our transient approach allowed us to observe the time segregation between DOC phytoplankton production and subsequent in situ bacterial degradation.

Contrary to the autumn, wind-driven circulation was very active during the winter survey. However, reduced light-limited phytoplankton production at this time of year precluded the intense DOC production/degradation cycle suggested by the  $O - I$  balance. DOC exchange across the boundaries of the study system is mainly due to changes in the standing stock of accumulated materials with recycling time larger than the flushing time.

*Implication for the carbon balance in upwelling regions*—The net consumption of inorganic carbon by the community of organisms in a given system transforms into  $\text{CaCO}_3$  and suspended, dissolved, and sedimented organic carbon. The almost 20-yr-old controversy on the fate of new organic materials produced in ocean margins, horizontal export versus in situ oxidation, has centered around organic particles and their direct sedimentation on the shelf or export to continental slope sediments (Walsh et al. 1988; Biscaye et al. 1994). In parallel to this discussion, many marine biogeochemists focused their efforts on the minor but very reactive fraction of the DOM pool that contributes to carbon cycling in the oceans. Although the key role played by bioreactive DOM is widely recognized nowadays (e.g., Kirchman et al. 1993; Carlson et al. 1994; Hansell and Carlson 1998), it has not been properly incorporated in the discussion about the fate of organics in continental shelves. The net production of bioreactive DOM adds a new possible fate for the new production in ocean margins: the horizontal export to the adjacent ocean surface waters. This new route has to be important in coastal upwelling regions, in which horizontal export is magnified by the offshore Ekman transport, especially at sites where filaments develop. In this sense, a large filament is recurrently observed off the Ría de Vigo during the upwelling season (Haynes et al. 1993). Our results indicate that  $\sim 20\%$  of the net primary production in the study volume transform into labile DOC during upwelling episodes. This number agrees very well with the 20% value assumed by Hansell and Carlson (1998) for coastal upwelling systems of the world ocean in their global estimates of the NEP of DOC. The fate of organic materials in the global coastal upwelling zone has to be revisited under the light of these recent estimates.

Labile DOC exported to the adjacent ocean surface waters

will ultimately serve as a substrate for growth and respiration of bacterial populations there. The impact of exported DOC to the activation of the microbial loop is especially important when the receptor ecosystem is oligotrophic. This is the case of the subtropical gyres surrounding the highly productive belt of the equatorial Pacific (Hansell and Waterhouse 1997). Therefore, horizontal export of labile DOC must also be considered in the recent controversy of the autotrophic (Williams 1998) or heterotrophic (Duarte and Agustí 1998) status of open ocean waters. Considering recent estimates (Hansell and Carlson 1998), global new production of coastal upwelling areas is  $0.8 \text{ Gt C yr}^{-1}$ . Under the assumption that 20% transforms into labile DOC,  $\sim 0.16 \text{ Gt C yr}^{-1}$  could be exported from coastal upwelling systems to the adjacent open ocean waters to fuel heterotrophic processes there.

## References

- ÁLVAREZ-SALGADO, M., D. DOVAL, AND F. F. PÉREZ. 1999. Dissolved organic matter in shelf waters off the Ría de Vigo (NW Iberian upwelling system). *J. Mar. Syst.* **18**: 383–394.
- ANDERSON, T. R., AND P. J. WILLIAMS. 1999. A one-dimensional model of dissolved organic carbon cycling in the water column incorporating combined biological-photochemical decomposition. *Global Biogeochem. Cycles* **13**: 337–349.
- BAKUN, A., AND C. S. NELSON. 1991. The seasonal cycle of wind-stress curl in subtropical eastern boundary current regions. *J. Phys. Oceanogr.* **21**: 1815–1834.
- BARBER, R. T., AND R. L. SMITH. 1981. Coastal upwelling ecosystems, p. 31–68. *In* A. R. Longhurst [ed.]. *Analysis of marine systems*. Academic.
- BISCAYE, P. E., C. N. FLAGG, AND P. G. FALKOWSKI. 1994. The shelf edge exchange processes experiment, SEEP-II: An introduction to hypothesis, results and conclusions. *Deep-Sea Res.* **41**: 231–252.
- BRONK, D. A., P. M. GLIBERT, AND B. B. WARD. 1994. Nitrogen uptake, dissolved organic nitrogen release, and new production. *Science* **265**: 1843–1846.
- CARLSON, C. A., H. W. DUCKLOW, AND A. F. MICHAELS. 1994. Annual flux of dissolved organic carbon from the euphotic zone in the North-western Sargasso Sea. *Nature* **371**: 405–408.
- CHANG, J., AND E. J. CARPENTER. 1985. Blooms of the dinoflagellate *Gyrodinium aureolum* in a Long Island estuary: Box model analysis of bloom maintenance. *Mar. Biol.* **89**: 83–93.
- COPIN-MONTÉGUT, G., AND B. AVRIL. 1993. Vertical distribution and temporal variation of dissolved organic carbon in the North Western Mediterranean Sea. *Deep-Sea Res.* **40**: 1963–1972.
- CULLEN, J. J., S. G. HERRIGAN, M. E. HUNTLEY, AND F. M. H. REID. 1982. Yellow water in La Jolla Bay, California, July 1980. I. A bloom of the dinoflagellate *Gymnodinium flavum* Kofoid and Swezy. *J. Exp. Mar. Biol. Ecol.* **63**: 67–80.
- DOVAL, M. D., X. A. ÁLVAREZ-SALGADO, AND F. F. PÉREZ. 1997. Dissolved organic matter cycling in a temperate embayment affected by coastal upwelling. *Mar. Ecol. Prog. Ser.* **157**: 21–37.
- DUARTE, C. M., AND S. AGUSTÍ. 1998. The  $\text{CO}_2$  balance of unproductive aquatic ecosystems. *Science* **281**: 234–236.
- EPPLEY, R. W., AND B. J. PETERSON. 1979. Particulate organic matter flux and planktonic new production in the deep ocean. *Nature* **282**: 677–680.
- FIGUEIRAS F. G., AND A. F. RÍOS. 1993. Phytoplankton succession, red tides and hydrographic regime in the Rías Bajas of Galicia, p. 239–244. *In*: T. J. Smayda and Y. Shimizu [eds]. *Toxic marine phytoplankton*. Elsevier.
- FUHRMAN, J. A. 1992. Bacterioplankton roles in cycling of organic matter: the microbial food web, p. 361–383. *In*: P. G. Falkowski and A. D. Woodhead [eds]. *Primary productivity and biogeochemical cycles in the sea*. Plenum.
- HANSELL, D. A., AND C. A. CARLSON. 1998. Net community production of dissolved organic carbon. *Global Biogeochem. Cycles* **12**: 443–453.
- , AND T. Y. WATERHOUSE. 1997. Control of the distributions of organic carbon and nitrogen in the eastern Pacific Ocean. *Deep-Sea Res.* **44**: 843–857.
- HAYNES, R., AND E. D. BARTON. 1990. A poleward flow along the Atlantic coast of the Iberian Peninsula. *J. Geophys. Res.* **95**: 11425–11441.
- , ———, AND I. PILLING. 1993. Development, persistence and variability of upwelling filaments off the Atlantic coast of the Iberian Peninsula. *J. Geophys. Res.* **98**: 22681–22692.
- KIRCHMAN, D. L., C. LANCELOT, M. FASHAM, L. LEGENDRE, G. RADACH, AND M. SCOTT. 1993. Dissolved organic material in biogeochemical models of the ocean, p. 209–225. *In* G. T. Evans and M. J. R. Fasham [eds.]. *Towards a model of ocean biogeochemical processes*. NATO series I: Global environmental change, 10. Springer Verlag.
- , Y. SUZUKI, C. GARSIDE, AND H. W. DUCKLOW. 1991. High turnover rates of dissolved organic carbon during a spring phytoplankton bloom. *Nature* **352**: 612–614.
- MONCOIFFÉ, G., X. A. ÁLVAREZ-SALGADO, G. SAVIDGE, AND F. G. FIGUEIRAS. 2000. Seasonal and short-time-scale dynamics of microplankton community production and respiration in an in-shore upwelling system. *Mar. Ecol. Prog. Ser.* **196**: 111–126.
- NOGUEIRA, E., F. F. PÉREZ, AND A. F. RÍOS. 1997. Seasonal and long-term trends in an estuarine upwelling ecosystem (Ría de Vigo, NW Spain). *Estuar. Coastal Shelf Sci.* **44**: 285–300.
- NORRMAN, B., U. L. ZWEIFEL, C. S. HOPKINSON, AND B. FRY. 1995. Production and utilisation of dissolved organic carbon during an experimental diatom bloom. *Limnol. Oceanogr.* **40**: 898–907.
- PÉREZ, F. F., X. A. ÁLVAREZ-SALGADO, AND G. ROSÓN. 2000. Stoichiometry of net ecosystem metabolism in coastal inlet affected by upwelling: the Ría de Arousa (NW Spain). *Mar. Chem.* **69**: 217–236.
- QUINONES, R. A., AND T. PLATT. 1991. The relationship between the F-ratio and the P:R ratio in the pelagic ecosystem. *Limnol. Oceanogr.* **36**: 211–213.
- ROSÓN, G., X. A. ÁLVAREZ-SALGADO, AND F. F. PÉREZ. 1997. A non-stationary box-model to determine residual flows in a partially mixed estuary, based on both thermohaline properties: application to the Ría de Arousa (NW Spain). *Estuar. Coastal Shelf Sci.* **44**: 249–262.
- SMITH, S. V., AND J. T. HOLLIBAUGH. 1997. Annual cycle and interannual variability of ecosystem metabolism in a temperate climate embayment. *Ecol. Monogr.* **67**: 509–533.
- THINGSTAD, T. F., A. HAGSTRÖM, AND F. RASSOULZADEGAN. 1997. Accumulation of degradable DOC in surface waters: is it caused by a malfunctioning microbial loop? *Limnol. Oceanogr.* **42**: 398–404.
- UNESCO. 1985. The international system of units (SI) in oceanography. UNESCO technical papers in marine sciences 45.
- WALSH, J. J., P. E. BISCAYE, AND G. T. CSANADY. 1988. The 1983–84 Shelf Edge Exchange Processes (SEEP)-I experiment: Hypothesis and highlights. *Cont. Shelf Res.* **8**: 35–56.
- , ———, AND ———. 1991. Importance of continental margins in the marine biogeochemical cycling of carbon and nitrogen. *Nature* **359**: 53–55.

- WILLIAMS, P. J. 1998. The balance of plankton respiration and photosynthesis in the open oceans. *Nature* **394**: 55–57.
- WOLLAST, R. 1993. Interactions of carbon and nitrogen cycles in the coastal zone, p. 195–210. *In* R. Wollast, F. T. Mackenzie, and L. Chou [eds.]. Interactions of C, N, P, and S biogeochemical cycles and global change. NATO Series I: Global Environmental Change, 4. Springer Verlag.
- WOOSTER, W. S., A. BAKUN, AND D. R. MCCLAIN. 1976. The seasonal upwelling cycle along the eastern boundary of the North Atlantic. *J. Mar. Res.* **34**: 131–141.

*Received: 1 December 1999*  
*Amended: 6 September 2000*  
*Accepted: 18 September 2000*